Inorganic Chemistry

pubs.acs.org/IC

Article

High-Pressure Synthesis of Quadruple Perovskite Oxide $CaCu_3Cr_2Re_2O_{12}$ with a High Ferrimagnetic Curie Temperature

Jie Zhang, Zhehong Liu, Xubin Ye, Xiao Wang, Dabiao Lu, Haoting Zhao, Maocai Pi, Chien-Te Chen, Jeng-Lung Chen, Chang-Yang Kuo, Zhiwei Hu, Xiaohui Yu, Xueqiang Zhang, Zhao Pan,* and Youwen Long*

Cite This: *Inorg. Chem.* 2024, 63, 3499−3505

Read Online

ACCESS | Metrics & More | Article Recommendations

ABSTRACT: An $AA'_3B_2B'_2O_{12}$-type quadruple perovskite oxide of $CaCu_3Cr_2Re_2O_{12}$ was synthesized at 18 GPa and 1373 K. Both an A- and B-site ordered quadruple perovskite crystal structure was observed, with the space group *Pn*-3. The valence states are verified to be $CaCu_3^{2+}Cr_2^{3+}Re_2^{5+}O_{12}$ by bond valence sum calculations and synchrotron X-ray absorption spectroscopy. The spin interaction among Cu^{2+}, Cr^{3+}, and Re^{5+} generates a ferrimagnetic transition with the Curie temperature (T_C) at about 360 K. Moreover, electric transport properties and specific heat data suggest the presence of a half-metallic feature for this compound. The present study provides a promising quadruple perovskite oxide with above-room-temperature ferrimagnetism and possible half-metallic properties, which shows potential in the usage of spintronic devices.

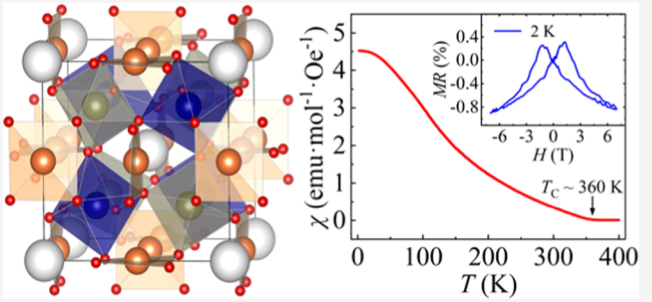

1. INTRODUCTION

Perovskite oxides with the chemical formula ABO_3 have attracted much attention due to their wide varieties of physical and chemical properties, such as ferromagnetism, ferroelectricity, multiferroic, superconductivity, negative thermal expansion, etc.[1−8] In ABO_3 perovskites, the A-site is typically occupied by large-size nonmagnetic alkali-metal, alkaline-earth, or lanthanide cations, while the B-site can be filled with various magnetic transition metals. Half of the B-site can be substituted by another transition metal B′. When the difference between the two kinds of transition-metal ions, including the ionic radii and the valence state, is large enough, the B-site ordered double perovskites (DPs) $A_2BB'O_6$ with a typical rocksalt type tend to form.[9] Sr_2FeMoO_6 is a representative DP material with intriguing half-metallic property.[10] On the other hand, three-quarter A-site cations can be substituted by small-size Jahn−Teller active ions such as Mn^{3+} ($t_{2g}^3e_g^1$) and Cu^{2+} ($t_{2g}^6e_g^3$), which tends to form a square-coordinated unit.[11,12] As a result, A-site ordered quadruple perovskites (QPs) with the chemical formula $AA'_3B_4O_{12}$ with heavily tilted BO_6 octahedra can be formed, and intriguing physical properties can therefore be expected. For example, typical QPs such as $CaCu_3Ti_4O_{12}$ with a large dielectric constant,[13] $LaCu_3Fe_4O_{12}$ exhibiting intermetallic charge transfer and unusual negative thermal expansion properties,[14] and multiferroic in $RMn_3Cr_4O_{12}$ (R = rare earth element and Bi)[15−18] have been extensively studied. One can suppose that the above two kinds of site orderings can be combined to design new materials of both A- and B-site ordered QPs with the chemical formula $AA'_3B_2B'_2O_{12}$. Owing to the multiple interactions of magnetic ions at various sites (A', B, and B' sites), such materials could show more intriguing physical properties, such as charge disproportionation, multiple magnetic transition, high-temperature magnetic ordering, high-performance half-metallicity, and so on.[19−23]

To date, although many simple ABO_3 perovskites and B-site ordered DPs have been reported, the study of $AA'_3B_2B'_2O_{12}$ perovskites is relatively limited because a unique high-pressure synthesis method is usually required to stabilize the heavily tilted octahedra in these QPs. Recently, Cr-based DPs have received increasing attention. Specifically, Cr-based ordered DPs A_2CrMO_6 (A = Sr, Ca; M = Mo, W, Re, Os) with ferromagnetic (FM) or ferrimagnetic (FiM) properties, in which Cr^{3+} ($3d^3$, S = 3/2) and Mo^{5+} ($4d^1$, S = 1/2) [W^{5+} ($5d^1$, S = 1/2), Re^{5+} ($5d^2$, S = 1), Os^{5+} ($5d^3$, S = 3/2)] couple antiferromagnetically, have been studied since the 1960s.[24] Then, B-site ordered DP Ca_2CrReO_6 was reported to be a FiM insulator with a T_C of 360 K, and metallic Sr_2CrReO_6 exhibited a higher T_C of 635 K.[25] Moreover, Sr_2CrOsO_6 has the highest

Received: November 29, 2023
Revised: January 13, 2024
Accepted: January 24, 2024
Published: February 6, 2024

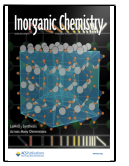

T_C of 725 K among DP oxide materials.[26] However, Cr-based A- and B-site ordered QPs with different magnetic ions at B/B′ sites have not been reported yet. In this paper, a new Cr-based A- and B-site ordered QP $CaCu_3Cr_2Re_2O_{12}$ (CCCRO) prepared using a high-pressure method was reported. Above-room-temperature ferrimagnetism accompanied by a possible half-metallic property was observed. The detailed crystal structure, valence state, and magnetic and transport properties were studied.

2. EXPERIMENTAL SECTION

The polycrystalline $CaCu_3Cr_2Re_2O_{12}$ was synthesized from stoichiometric mixtures of high-purity (>99.9%) CaO, CuO, Cr_2O_3, ReO_2, and Re_2O_7 powders. These reactants were thoroughly mixed with the mole ratio of 3:9:3:4:1, ground in an agate mortar, and then pressed into a gold capsule of 2.0 mm diameter and length within an argon-filled glovebox. The capsule was treated at 18 GPa and 1373 K for 45 min by using a Walker-type double-stage high-pressure apparatus. After heat treatment, the high pressure was slowly released to the ambient condition. Powder X-ray diffraction (XRD) was measured using a Huber diffractometer (Cu Kα_1 radiation, 40 kV, 20 mA) in the 2θ range from 10 to 100° at room temperature (RT). The data were refined by the Rietveld method using GSAS software.[27,28] The X-ray absorption spectroscopy (XAS) measurement at the Cu-$L_{2,3}$ and Cr-$L_{2,3}$ edges was carried out at RT using the total electron yield mode at the TLS11A beamline of the National Synchrotron Radiation Research Center (NSRRC) synchrotron facility in Taiwan. The XAS measurement at the Re-L_3 edge was performed at the TLS08A beamline of NSRRC with the transmission mode at RT. Magnetic susceptibility (χ) and magnetization (M) measurements were carried out using a superconducting quantum interference device magnetometer (Quantum Design, MPMS-VSM). Electrical transport with a standard four-probe method and specific heat properties were measured on a physical property measurement system (Quantum Design, PPMS-9 T).

3. RESULTS AND DISCUSSION

The XRD pattern and refinement results of the CCCRO compound are shown in Figure 1(a). The crystal indices of diffraction peaks with an odd-numbered total value $h + k + l$ [(111), (311), and (333)] in the XRD pattern indicate the rocksalt-type ordered arrangement of Cr/Re cations at the B/B' sites. Rietveld analysis suggested that CCCRO has both the A- and B-site ordered QP structure, the same as $CaCu_3Fe_2Re_2O_{12}$ with the space group Pn-3,[21] as shown in Figure 1(b). According to the refinements, the occupancy factors of both the A-site Ca and A'-site Cu atoms were close to 1.0, indicating that there was nearly neither Ca−Cu antisite occupancy nor other elements occupying these two sites due to their unique coordination environment. Therefore, these two occupancy factors were set to be unity. Note that an approximately 10.8% Cr−Re antisite occupancy was observed based on the refinement results. Combined with the expected valence states of the cations determined by XAS (see below), the oxygen vacancies can be ignored, and the occupancy factor of oxygen was fixed to be unity. The detailed structural parameters are listed in Table 1. As can be seen, four of the 12 Cu−O distances are short, 1.970 Å, indicating the square-planar coordination of oxygen around the A' site. According to the refined bond lengths, the bond valence sum (BVS) calculations indicate the valence states of Cu, Cr, and Re to be +2.15, + 2.79, and +5.04, respectively, suggesting a $CaCu_3^{2+}Cr_2^{3+}Re_2^{5+}O_{12}$ charge combination, in agreement with the XAS measurements shown below.

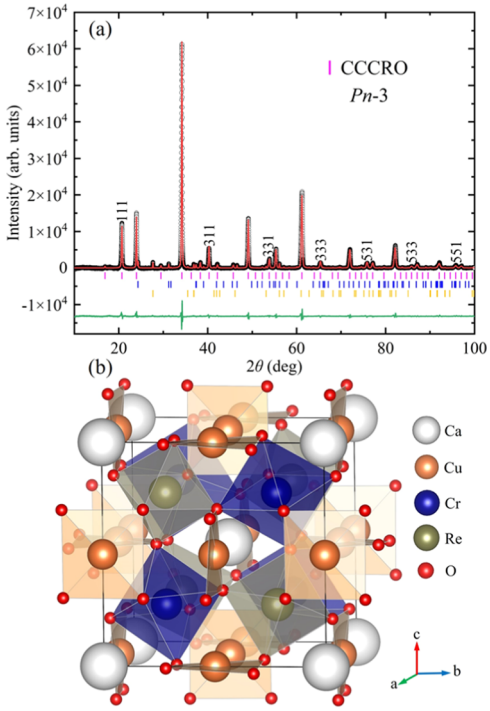

Figure 1. (a) XRD pattern and Rietveld refinement results of CCCRO at RT. The observed (black circles), calculated (red line), and difference (green line) are shown. The top ticks indicate the allowed Bragg reflections with the space group Pn-3. The middle and bottom ticks present a small amount of ReO_2 and CrOOH impurity phases (~5.7 wt % in total), respectively. (b) Schematic crystal structure with the space group Pn-3 for CCCRO.

To further confirm the valence states, we performed XAS measurements at the Cu-$L_{2,3}$, Cr-$L_{2,3}$, and Re-L_3 edges. Figure 2(a) shows the Cu-$L_{2,3}$ XAS of CCCRO together with that of $CaCu_3Ti_4O_{12}$ as a Cu^{2+} reference in a QP structure.[29] The similar shape of the peak and energy position indicates the formation of a Cu^{2+} valence state in CCCRO with a square-planar local environment. Figure 2(b) shows the Cr-$L_{2,3}$ XAS with $BiMn_3Cr_4O_{12}$ as a Cr^{3+} reference with a similar CrO_6 octahedral coordination environment.[16] The multiple spectral features and energy positions of CCCRO are consistent with those of the Cr^{3+} reference, indicating the Cr^{3+} valence state at the octahedral B-site. The Re-L_3 XAS of CCCRO, Sr_2MgReO_6 as a Re^{6+} reference,[30] and Sr_2FeReO_6 as a Re^{5+} reference[31] are shown in Figure 2(c). The Re-L_3 of CCCRO shifts more than 1 eV to a lower energy compared with that of the Re^{6+} reference but locates at a similar energy with that of the Re^{5+} reference, which indicates the formation of the Re^{5+} valence state. Therefore, the XAS measurements of CCCRO confirm the charge combination to be $CaCu_3^{2+}Cr_2^{3+}Re_2^{5+}O_{12}$.

Figure 3(a) shows the temperature dependence of the dc magnetic susceptibility of CCCRO from 2 to 400 K in the field cooling mode under an external field of 0.1 T. With decreasing temperature, the susceptibility experiences an increase at the onset of about 360 K, which is more clearly visible in the curve of the temperature dependence of the first derivative of magnetic susceptibility [see the inset of Figure 3(a)], suggesting an FM-like transition as demonstrated by the field-dependent magnetization shown in Figure 3(b), where noticeable magnetic hysteresis behavior can be observed below T_C. The FM-like magnetic transition cannot be attributed to

https://doi.org/10.1021/acs.inorgchem.3c04243
Inorg. Chem. 2024, 63, 3499−3505

Table 1. Structure Parameters and BVS Results of CCCRO Refined from the XRD Pattern at RT[a]

parameter	CCCRO
a (Å)	7.4152(2)
O_x	0.5583(6)
O_y	0.7559(3)
O_z	0.0662(6)
G (2a for Ca)	1.0
G (6d for Cu)	1.0
G (4b for Cr1)	0.892(1)
G (4b for Re1)	0.108(1)
G (4c for Re2)	0.892(1)
G (4c for Cr2)	0.108(1)
G (24h for O)	1.0
U_{iso} (Ca) (100 × Å^2)	0.8(3)
U_{iso} (Cu) (100 × Å^2)	1.7(1)
U_{iso} (Cr1) (100 × Å^2)	0.4(3)
U_{iso} (Re2) (100 × Å^2)	1.2(4)
U_{iso} (O) (100 × Å^2)	0.7(1)
Cu−O (×4) (Å)	1.970(3)
Cr1−O (×6) (Å)	2.007(2)
Re2−O (×6) (Å)	1.924(2)
∠Cr1−O−Re2 (°)	141.1(1)
∠Cu−O−Cr1 (°)	107.7(1)
∠Cu−O−Re2 (°)	111.1(1)
BVS (Cu)	2.15
BVS (Cr)	2.79
BVS (Re)	5.04
R_{wp} (%)	4.92
R_p (%)	3.36

[a]Crystal data: space group Pn-3 (No. 201); atomic sites: Ca 2a (0.25, 0.25, 0.25); Cu 6d (0.25, 0.75, 0.75); Cr 4b (0, 0, 0); Re 4c (0.5, 0.5, 0.5); O 24h (x, y, z). The BVS values (V_i) were calculated using the formula $V_i = \sum_j S_{ij}$ and $S_{ij} = \exp[(r_0 - r_{ij})/0.37]$. The values of r_0 were 1.679 for Cu, 1.724 for Cr, and 1.86 for Re. For the B-site Cr and B'-site Re, six coordinated oxygen atoms were used. For the A'-site Cu, 12 coordinated oxygen atoms were used. G, site occupancy.

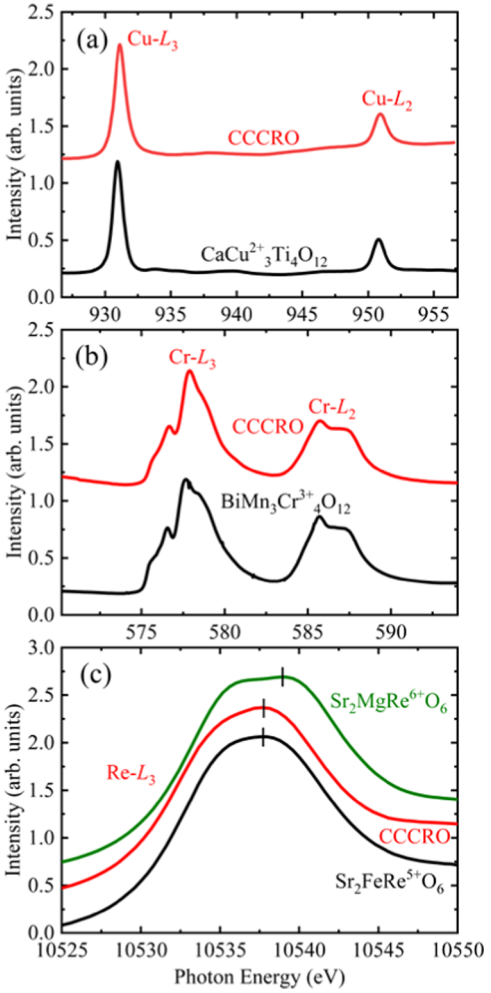

Figure 2. XAS of (a) Cu-$L_{2,3}$ edges, (b) Cr-$L_{2,3}$ edges, and (c) Re-L_3 edges for CCCRO. The XASs of some related references are also shown for comparison.

detectable impurities ReO_2 and CrOOH [illustrated in Figure 1(a)] due to their paramagnetic property and antiferromagnetic transition with a lower Néel temperature, respectively.[32,33] The T_C of CCCRO is lower than that of $CaCu_3Fe_2Re_2O_{12}$.[21] Considering the nearly identical structural parameters of these compounds, the reduction in T_C primarily results from the decrease of the number of unpaired d-electrons in a Cr^{3+} ion compared to an Fe^{3+} ion, which weakens the superexchange spin interactions of B−O−Re. However, the magnetic interactions are enhanced compared to $CaCu_3Cr_2Sb_2O_{12}$[34] due to the existence of magnetic ions at the B' site. The shape of the $\chi(T)$ curve in Figure 3(a) illustrates a broad FM or FiM transition, indicating a certain degree of anisotropy in this sample or the presence of a competing magnetic interaction. The latter may originate from the short-range correlation by the B-site antisite defect. As shown in Figure 4(b), there is no clear anomaly in the specific heat around T_C, which also suggests the occurrence of short-range correlation and/or competing magnetic interaction. The magnetization at 2 K shows remarkable magnetic hysteresis with a coercive field of about 1 T [Figure 3(b)], which is reminiscent of hard magnetic materials; however, the B-site disordered defect can also result in a certain degree of hysteresis. The saturated moment is about 1.6 μ_B per formula unit (f.u.) at 2 K, which is relatively small compared to other A- and B-site ordered FiM QPs.[21−23]

In the currently available A- and B-site ordered QPs with the A' site occupied by Cu ions and B/B' sites occupied by magnetic ions, a single magnetic transition driven by the different sites of magnetic ions can usually be observed.[21−23] The spin arrangement is usually Cu(↑)B(↑)B'(↓) with strong Cu(↑)B'(↓) and B(↑)B'(↓) antiferromagnetic (AFM) coupling through a superexchange interaction (B and B' represent 3d and 5d transition-metal ions, respectively); the Cu(↑)B(↓) AFM coupling is relatively weak. As a result, the Cu(↑)B(↑) FM arrangement appears, followed by the magnetic frustration in these systems. For the origin of magnetism in CCCRO, if spin-only interactions are considered, the moments of Cu^{2+}, Cr^{3+}, and Re^{5+} are M_{Cu} = 1.0 μ_B, M_{Cr} = 3.0 μ_B, and M_{Re} = 2.0 μ_B, respectively. However, in this case, Cu(↑)Cr(↑)Re(↑), Cu(↑)Cr(↓)Re(↓), and Cu(↑)Cr(↓)Re(↑) alignments show unreasonable moment values compared with the experiment. Even though the Cu(↑)Cr(↑)Re(↓) configuration (5.0 μ_B/f.u.) shows the most reasonable value, it is still much larger than the experimental result (1.6 μ_B/f.u.). The magnetic properties seem to be strongly influenced by the assumed configuration of the B/B'-site Cr/Re arrangement, while the nominal valences remain unaffected. This phenomenon is well documented in DP families, in which the moment decreases with the increase

https://doi.org/10.1021/acs.inorgchem.3c04243
Inorg. Chem. 2024, 63, 3499−3505

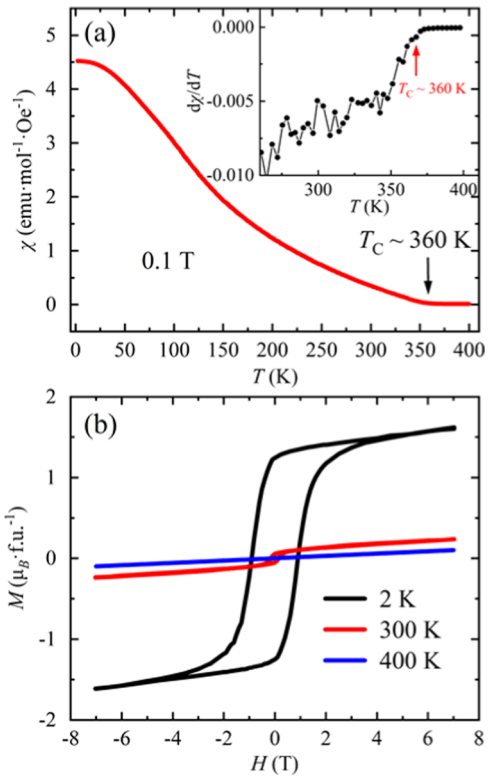

Figure 3. (a) Temperature dependence of magnetic susceptibility measured at 0.1 T with the FC mode for CCCRO. The inset shows the temperature dependence of the first derivative of magnetic susceptibility. (b) Field dependence of magnetization measured at different temperatures for CCCRO.

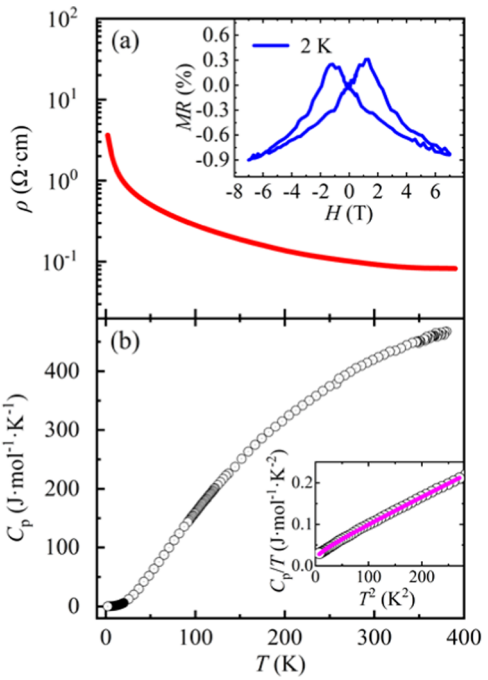

Figure 4. (a) Temperature dependence of resistivity at zero magnetic field for CCCRO. The inset shows the field-dependent MR effects measured at 2 K. (b) Temperature dependence of specific heat at zero field for CCCRO. The inset shows the fitting result of specific heat below 17 K using the function $C_p/T = \gamma + \beta T^2 + \alpha T^{1/2}$, yielding γ = 6.4(1) mJ/mol·K^2, β = 0.60(5) mJ/mol·K^4, and α = 10.3(6) mJ/mol·K$^{5/2}$.

of disorder.[35] Moreover, in this case, although the strength of the dominant magnetic Cu−Re and Cr−Re interactions is slightly affected, the disordered arrangement of the Cr/Re ions could introduce significant competition and uncertainty in spin orientations at the B and B' sites. As a result, the magnetic frustration is markedly enhanced in the present sample.[36] This could explain the suppression of the saturated moment of 1.6 μ_B/f.u. contrasting with the theoretical value of 5.0 μ_B/f.u. in a perfectly ordered state.

In order to study the electrical transport properties of CCCRO, the temperature dependence of resistivity from 2 to 390 K and magnetoresistance effects [MR = 100% × ($\rho(H) - \rho(0)$)/$\rho(0)$] at 2 K were measured. The resistivity is at the level of 10^{-1} Ω cm at 390 K, and it slightly increases to about 3.7 Ω cm at 2 K upon cooling, as shown in Figure 4(a). The low-temperature specific heat of CCCRO can be well fitted using the function $C_p/T = \gamma + \beta T^2 + \alpha T^{1/2}$ [see the inset of Figure 4(b)], yielding γ = 6.4(1) mJ/mol·K^2, β = 0.60(5) mJ/mol·K^4, and α = 10.3(6) mJ/mol·K$^{5/2}$. The presence of contribution of electrons can be obtained, as reflected by the fitted Sommerfeld coefficient γ = 6.4(1) mJ/mol·K^2. Considering the polycrystalline nature of CCCRO, where grain boundary scattering effects play some roles in resistance, the weak temperature dependence of resistivity may imply metallic conductivity. Notably, a butterfly-shaped MR curve can be observed at 2 K [Figure 4(a)]. This feature typically arises from intergrain tunneling of the spin-polarized conduction electrons.[10,37] Note that the hysteresis field of MR (1.5 T) is larger than that of magnetization (1.0 T), indicating a spin-valve-type MR arising from the intergrain tunneling for the spin-polarized carriers.[38] This could imply a half-metallic property. Similar phenomena were also observed in the half-metallic QPs $CaCu_3Fe_2Re_2O_{12}$, $LaCu_3Co_2Re_2O_{12}$, and $LaCu_3Fe_2Re_2O_{12}$.[21−23] In these 3d−5d strongly hybridized systems, a robust Cu−B−B' covalent network can form through intervening oxygens. This network, facilitated by strong Cu−O−B and B−O−B' pathway hybridizations, leads to the previously discussed strong Cu(↑)B(↑)B'(↓) magnetic coupling. The extended Re t_{2g} orbitals, with weak electron correlation effects, dominate the electronic states near the Fermi level and exhibit spin polarization.[39] This results in a metallic property in the down (minority) spin channel owing to the partially filled t_{2g} down spin orbitals. In the up (majority) spin channel, the 3d electrons of B and Cu, showing strong electron correlation effects, tend to favor a Mott insulating state. Furthermore, in CCCRO, the t_{2g} up spin orbitals of Cr^{3+} are fully filled, tending to create a substantial energy gap in this channel. Therefore, in comparison to QPs $ACu_3Fe_2Re_2O_{12}$[21,23,39] with a similar crystal structure, as well as DPs Sr_2FeReO_6 and Sr_2CrReO_6[40−42] with a comparable electronic configuration, the half-metallic property is expected to occur in the present CCCRO. The MR value of CCCRO at 2 K and 7 T is less than 1%; the relatively small value is related to the strong magnetic frustration, as well as the small amount of Cr/Re disorder effects.[43]

4. CONCLUSIONS

In summary, a new Cr-based QP oxide CCCRO has been synthesized by using the high-pressure method. The CCCRO QP compound shows both the A- and B-site ordered perovskite structure with the space group *Pn*-3. The valence states and local environment of Cu, Cr, and Re were studied by

https://doi.org/10.1021/acs.inorgchem.3c04243
Inorg. Chem. 2024, 63, 3499−3505

the XAS techniques, revealing a square-planar coordination of $Cu^{2+}O_4$ at the A' site and an octahedral coordination of $Cr^{3+}O_6$ ($Re^{5+}O_6$) at the B (B') site, with the charge combination of $CaCu_3^{2+}Cr_2^{3+}Re_2^{5+}O_{12}$. A high T_C above room temperature of about 360 K is observed due to the magnetic coupling between the transition-metal cations. Most intriguingly, the electric transport measurements suggest that the CCCRO compound exhibits half-metallic properties. The combination of high T_C and half-metallicity in the current CCCRO demonstrates its potential applications in spintronic devices.

AUTHOR INFORMATION

Corresponding Authors

Zhao Pan − *Beijing National Laboratory for Condensed Matter Physics, Institute of Physics, Chinese Academy of Sciences, Beijing 100190, China; School of Physical Sciences, University of Chinese Academy of Sciences, Beijing 100049, China;* orcid.org/0000-0002-8693-2508; Email: zhaopan@iphy.ac.cn

Youwen Long − *Beijing National Laboratory for Condensed Matter Physics, Institute of Physics, Chinese Academy of Sciences, Beijing 100190, China; School of Physical Sciences, University of Chinese Academy of Sciences, Beijing 100049, China; Songshan Lake Materials Laboratory, Dongguan 523808 Guangdong, China;* orcid.org/0000-0002-8587-7818; Email: ywlong@iphy.ac.cn

Authors

Jie Zhang − *Beijing National Laboratory for Condensed Matter Physics, Institute of Physics, Chinese Academy of Sciences, Beijing 100190, China; School of Physical Sciences, University of Chinese Academy of Sciences, Beijing 100049, China;* orcid.org/0009-0006-9055-2969

Zhehong Liu − *Beijing National Laboratory for Condensed Matter Physics, Institute of Physics, Chinese Academy of Sciences, Beijing 100190, China*

Xubin Ye − *Beijing National Laboratory for Condensed Matter Physics, Institute of Physics, Chinese Academy of Sciences, Beijing 100190, China;* orcid.org/0000-0002-5739-8318

Xiao Wang − *Beijing National Laboratory for Condensed Matter Physics, Institute of Physics, Chinese Academy of Sciences, Beijing 100190, China;* orcid.org/0000-0001-8139-4192

Dabiao Lu − *Beijing National Laboratory for Condensed Matter Physics, Institute of Physics, Chinese Academy of Sciences, Beijing 100190, China; School of Physical Sciences, University of Chinese Academy of Sciences, Beijing 100049, China;* orcid.org/0009-0006-5489-2835

Haoting Zhao − *Beijing National Laboratory for Condensed Matter Physics, Institute of Physics, Chinese Academy of Sciences, Beijing 100190, China; College of Materials Science and Opto-Electronic Technology, University of Chinese Academy of Sciences, Beijing 100049, China;* orcid.org/0009-0007-9656-5709

Maocai Pi − *Beijing National Laboratory for Condensed Matter Physics, Institute of Physics, Chinese Academy of Sciences, Beijing 100190, China; School of Physical Sciences, University of Chinese Academy of Sciences, Beijing 100049, China*

Chien-Te Chen − *National Synchrotron Radiation Research Center, Hsinchu 30076, Taiwan*

Jeng-Lung Chen − *National Synchrotron Radiation Research Center, Hsinchu 30076, Taiwan*

Chang-Yang Kuo − *National Synchrotron Radiation Research Center, Hsinchu 30076, Taiwan; Department of Electrophysics, National Yang Ming Chiao Tung University, Hsinchu 30010, Taiwan*

Zhiwei Hu − *Max Planck Institute for Chemical Physics of Solids, Dresden 01187, Germany;* orcid.org/0000-0003-0324-2227

Xiaohui Yu − *Beijing National Laboratory for Condensed Matter Physics, Institute of Physics, Chinese Academy of Sciences, Beijing 100190, China; School of Physical Sciences, University of Chinese Academy of Sciences, Beijing 100049, China;* orcid.org/0000-0001-8880-2304

Xueqiang Zhang − *Beijing National Laboratory for Condensed Matter Physics, Institute of Physics, Chinese Academy of Sciences, Beijing 100190, China; School of Physical Sciences, University of Chinese Academy of Sciences, Beijing 100049, China*

Complete contact information is available at: https://pubs.acs.org/10.1021/acs.inorgchem.3c04243

Notes

The authors declare no competing financial interest.

ACKNOWLEDGMENTS

This work was supported by the National Key R&D Program of China (Grant No. 2021YFA1400300), the National Natural Science Foundation of China (Grant Nos. 12261131499, 11934017, 11921004, 22271309, 12204516, 12304159, 12304268, and 21805215), the Beijing Natural Science Foundation (Grant No. Z200007), and the Chinese Academy of Sciences (Grant No. XDB33000000). The authors acknowledge the support from the Max Planck-POSTECH-Hsinchu Center for Complex Phase Materials.

REFERENCES

(1) Cava, R. J.; Batlogg, B.; Van Dover, R. B.; Murphy, D. W.; Sunshine, S.; Siegrist, T.; Remeika, J. P.; Rietman, E. A.; Zahurak, S.; Espinosa, G. P. Bulk superconductivity at 91 K in single-phase oxygen-deficient perovskite $Ba_2YCu_3O_{9-\delta}$. *Phys. Rev. Lett.* **1987**, *58*, 1676.

(2) Cohen, R. E. Origin of ferroelectricity in perovskite oxides. *Nature* **1992**, *358*, 136.

(3) Salamon, M. B.; Jaime, M. The Physics of manganites: Structure and transport. *Rev. Mod. Phys.* **2001**, *73*, 583.

(4) Kimura, T.; Goto, T.; Shintani, H.; Ishizaka, K.; Arima, T.; Tokura, Y. Magnetic control of ferroelectric polarization. *Nature* **2003**, *426*, 55.

(5) Wang, J.; Neaton, J. B.; Zheng, H.; Nagarajan, V.; Ogale, S. B.; Liu, B.; Viehland, D.; Vaithyanathan, V.; Schlom, D. G.; Waghmare, U. V.; Spaldin, N. A.; Rabe, K. M.; Wuttig, M.; Ramesh, R. Epitaxial $BiFeO_3$ multiferroic thin film heterostructures. *Science* **2003**, *299*, 1719.

(6) Reyren, N.; Thiel, S.; Caviglia, A. D.; Kourkoutis, L. F.; Hammerl, G.; Richter, C.; Schneider, C. W.; Kopp, T.; Rüetschi, A.-S.; Jaccard, D.; Gabay, M.; Muller, D. A.; Triscone, J.-M.; Mannhart, J. Superconducting interfaces between insulating oxides. *Science* **2007**, *317*, 1196.

(7) Azuma, M.; Chen, W. T.; Seki, H.; Czapski, M.; Olga, S.; Oka, K.; Mizumaki, M.; Watanuki, T.; Ishimatsu, N.; Kawamura, N.; Ishiwata, S.; Tucker, M. G.; Shimakawa, Y.; Attfield, J. P. Colossal negative thermal expansion in $BiNiO_3$ induced by intermetallic charge transfer. *Nat. Commun.* **2011**, *2*, No. 347, DOI: 10.1038/ncomms1361.

(8) Liu, Z.; Sakai, Y.; Yang, J.; Li, W.; Liu, Y.; Ye, X.; Qin, S.; Chen, J.; Agrestini, S.; Chen, K.; Liao, S. C.; Haw, S. C.; Baudelet, F.; Ishii, H.; Nishikubo, T.; Ishizaki, H.; Yamamoto, T.; Pan, Z.; Fukuda, M.; Ohashi, K.; Matsuno, K.; Machida, A.; Watanuki, T.; Kawaguchi, S. I.; Arevalo-Lopez, A. M.; Jin, C.; Hu, Z.; Attfield, J. P.; Azuma, M.; Long, Y. Sequential spin state transition and intermetallic charge transfer in $PbCoO_3$. *J. Am. Chem. Soc.* **2020**, *142*, 5731.
(9) Vasala, S.; Karppinen, M. $A_2B'B''O_6$ perovskites: A review. *Prog. Solid State Chem.* **2015**, *43*, 1.
(10) Kobayashi, K. I.; Kimura, T.; Sawada, H.; Terakura, K.; Tokura, Y. Room-temperature magnetoresistance in an oxide material with an ordered double-perovskite structure. *Nature* **1998**, *395*, 677.
(11) Long, Y.; Saito, T.; Mizumaki, M.; Agui, A.; Shimakawa, Y. Various valence states of square-coordinated Mn in A-site-ordered perovskites. *J. Am. Chem. Soc.* **2009**, *131*, 16244 DOI: 10.1021/ja906668c.
(12) Ye, X.; Song, S.; Li, L.; Chang, Y. C.; Qin, S.; Liu, Z.; Huang, Y. C.; Zhou, J.; Zhang, L. J.; Dong, C. L.; Pao, C. W.; Lin, H. J.; Chen, C. T.; Hu, Z.; Wang, J. Q.; Long, Y. A'−B intersite cooperation-enhanced water splitting in quadruple perovskite oxide $CaCu_3Ir_4O_{12}$. *Chem. Mater.* **2021**, *33*, 9295.
(13) Ramirez, A. P.; Subramanian, M. A.; Gardel, M.; Blumberg, G.; Li, D.; Vogt, T.; Shapiro, S. M. Giant dielectric constant response in a copper-titanate. *Solid State Commun.* **2000**, *115*, 217.
(14) Long, Y.; Hayashi, N.; Saito, T.; Azuma, M.; Muranaka, S.; Shimakawa, Y. Temperature-induced A−B intersite charge transfer in an A-site-ordered $LaCu_3Fe_4O_{12}$ perovskite. *Nature* **2009**, *458*, 60.
(15) Wang, X.; Chai, Y.; Zhou, L.; Cao, H.; Cruz, C. D.; Yang, J.; Dai, J.; Yin, Y.; Yuan, Z.; Zhang, S.; Yu, R.; Azuma, M.; Shimakawa, Y.; Zhang, H.; Dong, S.; Sun, Y.; Jin, C.; Long, Y. Observation of magnetoelectric multiferroicity in a cubic perovskite system: $LaMn_3Cr_4O_{12}$. *Phys. Rev. Lett.* **2015**, *115*, No. 087601, DOI: 10.1103/PhysRevLett.115.087601.
(16) Zhou, L.; Dai, J.; Chai, Y.; Zhang, H.; Dong, S.; Cao, H.; Calder, S.; Yin, Y.; Wang, X.; Shen, X.; Liu, Z.; Saito, T.; Shimakawa, Y.; Hojo, H.; Ikuhara, Y.; Azuma, M.; Hu, Z.; Sun, Y.; Jin, C.; Long, Y. Realization of large electric polarization and strong magnetoelectric coupling in $BiMn_3Cr_4O_{12}$. *Adv. Mater.* **2017**, *29*, No. 1703435, DOI: 10.1002/adma.201703435.
(17) Liu, G.; Liu, Z.; Chai, Y.; Zhou, L.; Shen, X.; Ye, X.; Qin, S.; Lu, D.; Hu, Z.; Tjeng, L. H.; Lin, H. J.; Chen, C. T.; Yu, X.; Long, Y. Magnetic and electric field dependent anisotropic magnetoelectric multiferroicity in $SmMn_3Cr_4O_{12}$. *Phys. Rev. B* **2021**, *104*, No. 054407.
(18) Liu, G.; Pi, M.; Zhou, L.; Liu, Z.; Shen, X.; Ye, X.; Qin, S.; Mi, X.; Chen, X.; Zhao, L.; Zhou, B.; Guo, J.; Yu, X.; Chai, Y.; Weng, H.; Long, Y. Physical realization of topological Roman surface by spin-induced ferroelectric polarization in cubic lattice. *Nat. Commun.* **2022**, *13*, No. 2373, DOI: 10.1038/s41467-022-29764-w.
(19) Yamada, I.; Takata, K.; Hayashi, N.; Shinohara, S.; Azuma, M.; Mori, S.; Muranaka, S.; Shimakawa, Y.; Takano, M. A perovskite containing quadrivalent iron as a charge-disproportionated ferrimagnet. *Angew. Chem., Int. Ed.* **2008**, *120*, 7140−7143, DOI: 10.1002/ange.200801482.
(20) Yin, Y. Y.; Liu, M.; Dai, J. H.; Wang, X.; Zhou, L.; Cao, H.; Cruz, C. D.; Chen, C. T.; Xu, Y.; Shen, X.; Yu, R.; Alonso, J. A.; Muñoz, A.; Yang, Y. F.; Jin, C.; Hu, Z.; Long, Y. $LaMn_3Ni_2Mn_2O_{12}$: An A-and B-site ordered quadruple perovskite with A-site tuning orthogonal spin ordering. *Chem. Mater.* **2016**, *28*, No. 8988, DOI: 10.1021/acs.chemmater.6b03785.
(21) Chen, W. T.; Mizumaki, M.; Seki, H.; Senn, M. S.; Saito, T.; Kan, D.; Attfield, J. P.; Shimakawa, Y. A half-metallic A-and B-site-ordered quadruple perovskite oxide $CaCu_3Fe_2Re_2O_{12}$ with large magnetization and a high transition temperature. *Nat. Commun.* **2014**, *5*, No. 3909, DOI: 10.1038/ncomms4909.
(22) Liu, Z.; Sun, Q.; Ye, X.; Wang, X.; Zhou, L.; Shen, X.; Chen, K.; Nataf, L.; Baudelet, F.; Agrestini, S.; Chen, C. T.; Lin, H. J.; Vasili, H. B.; Valvidares, M.; Hu, Z.; Yang, Y. F.; Long, Y. Quadruple perovskite oxide $LaCu_3Co_2Re_2O_{12}$: A ferrimagnetic half metal with nearly 100% B-site degree of order. *Appl. Phys. Lett.* **2020**, *117*, No. 152402, DOI: 10.1063/5.0025704.
(23) Liu, Z.; Zhang, S.; Wang, X.; Ye, X.; Qin, S.; Shen, X.; Lu, D.; Dai, J.; Cao, Y.; Chen, K.; Radu, F.; Wu, W. B.; Chen, C. T.; Francoual, S.; Mardegan, J. R. L.; Leupold, O.; Tjeng, L. H.; Hu, Z.; Yang, Y. F.; Long, Y. Realization of a half metal with a record-high Curie temperature in perovskite oxides. *Adv. Mater.* **2022**, *34*, No. 2200626, DOI: 10.1002/adma.202200626.
(24) Patterson, F. K.; Moeller, C. W.; Ward, R. Magnetic oxides of molybdenum (V) and tungsten (V) with the ordered perovskite structure. *Inorg. Chem.* **1963**, *2*, 196.
(25) Kato, H.; Okuda, T.; Okimoto, Y.; Tomioka, Y.; Takenoya, Y.; Ohkubo, A.; Kawasaki, M.; Tokura, Y. Metallic ordered double-perovskite Sr_2CrReO_6 with maximal Curie temperature of 635 K. *Appl. Phys. Lett.* **2002**, *81*, 328−330, DOI: 10.1063/1.1493646.
(26) Krockenberger, Y.; Mogare, K.; Reehuis, M.; Tovar, M.; Jansen, M.; Vaitheeswaran, G.; Kanchana, V.; Bultmark, F.; Delin, A.; Wilhelm, F.; Rogalev, A.; Winkler, A.; Alff, L. Sr_2CrOsO_6: End point of a spin-polarized metal-insulator transition by 5*d* band filling. *Phys. Rev. B* **2007**, *75*, No. 020404.
(27) Rietveld, H. A profile refinement method for nuclear and magnetic structures. *J. Appl. Crystallogr.* **1969**, *2*, 65−71, DOI: 10.1107/S0021889869006558.
(28) Toby, B. EXPGUI, a graphical user interface for GSAS. *J. Appl. Crystallogr.* **2001**, *34*, 210.
(29) McGuinness, C.; Downes, J. E.; Sheridan, P.; Glans, P. A.; Smith, K. E.; Si, W.; Johnson, P. D. X-ray spectroscopic study of the electronic structure of the high-dielectric-constant material $CaCu_3Ti_4O_{12}$. *Phys. Rev. B* **2005**, *71*, No. 195111.
(30) Wiebe, C. R.; Greedan, J. E.; Kyriakou, P. P.; Luke, G. M.; Gardner, J. S.; Fukaya, A.; Gat-Malureanu, I. M.; Russo, P. L.; Savici, A. T.; Uemura, Y. J. Frustration-driven spin freezing in the S = 1/2 fcc perovskite Sr_2MgReO_6. *Phys. Rev. B* **2003**, *68*, No. 134410.
(31) Herrero-Martín, J.; Subías, G.; Blasco, J.; García, J.; Sánchez, M. C. X-ray absorption spectroscopic study on A_2FeReO_6 double perovskites. *J. Phys.: Condens. Matter* **2005**, *17*, 4963.
(32) Hirai, D.; Anbai, T.; Uji, S.; Oguchi, T.; Hiroi, Z. Extremely large magnetoresistance in the hourglass Dirac loop chain metal β-ReO_2. *J. Phys. Soc. Jpn.* **2021**, *90*, No. 094708.
(33) Christensen, A. N. Hydrothermal preparation and magnetic properties of α-CrOOH, β-CrOOH and γ-CrOOH. *Acta Chem. Scand.* **1976**, *30a*, No. 133, DOI: 10.3891/ACTA.CHEM.SCAND.30A-0133.
(34) Byeon, S. H.; Lee, S. S.; Parise, J. B.; Woodward, P. M.; Hur, N. H. New ferrimagnetic oxide $CaCu_3Cr_2Sb_2O_{12}$: high-pressure synthesis, structure, and magnetic properties. *Chem. Mater.* **2005**, *17*, 3552.
(35) Saha-Dasgupta, T.; Sarma, D. D. ab initio study of disorder effects on the electronic and magnetic structure of Sr_2FeMoO_6. *Phys. Rev. B* **2001**, *64*, No. 064408.
(36) Senn, M. S.; Chen, W. T.; Saito, T.; Susana, G. M.; Attfield, J. P.; Shimakawa, Y. B-cation order control of magnetism in the 1322 perovskite $CaCu_3Fe_2Nb_2O_{12}$. *Chem. Mater.* **2014**, *26*, 4832−4837, DOI: 10.1021/cm502064b.
(37) Hwang, H. Y.; Cheong, S. W.; Ong, N. P.; Batlogg, A. B. Spin-polarized intergrain tunneling in $La_{2/3}Sr_{1/3}MnO_3$. *Phys. Rev. Lett.* **1996**, *77*, 2041.
(38) Sarma, D. D.; Ray, S.; Tanaka, K.; Kobayashi, M.; Fujimori, A.; Sanyal, P.; Krishnamurthy, H. R.; Dasgupta, C. Intergranular magnetoresistance in Sr_2FeMoO_6 from a magnetic tunnel barrier mechanism across grain boundaries. *Phys. Rev. Lett.* **2007**, *98*, No. 157205.
(39) Wang, D.; Shaikh, M.; Ghosh, S.; Sanyal, B. Prediction of half-metallic ferrimagnetic quadruple perovskites $ACu_3Fe_2Re_2O_{12}$ (A= Ca, Sr, Ba, Pb, Sc, Y, La) with high Curie temperatures. *Phys. Rev. Mater.* **2021**, *5*, No. 054405.
(40) Kato, H.; Okuda, T.; Okimoto, Y.; Tomioka, Y.; Oikawa, K.; Kamiyama, T.; Tokura, Y. Structural and electronic properties of the

ordered double perovskites A_2MReO_6 (A = Sr, Ca; M = Mg, Sc, Cr, Mn, Fe, Co, Ni, Zn). *Phys. Rev. B* **2004**, *69*, No. 184412.
(41) Kobayashi, K.-I.; Kimura, T.; Tomioka, Y.; Sawada, H.; Terakura, K.; Tokura, Y. Intergrain tunneling magnetoresistance in polycrystals of the ordered double perovskite Sr_2FeReO_6. *Phys. Rev. B* **1999**, *59*, No. 11159, DOI: 10.1103/PhysRevB.59.11159.
(42) Guo, S. Electronic structures of the ferrimagnetic double-perovskites Sr_2XReO_6 (X = Cr, Mn, Fe, Ni) with the modified Becke-Johnson potential. *Eur. Phys. J. B* **2015**, *88*, No. 82, DOI: 10.1140/epjb/e2015-50883-1.
(43) Wang, X.; Liu, M.; Shen, X.; Liu, Z.; Hu, Z.; Chen, K.; Ohresser, P.; Nataf, L.; Baudelet, F.; Lin, H. J.; Chen, C. T.; Soo, Y. L.; Yang, Y. F.; Long, Y. High-temperature ferrimagnetic half metallicity with wide spin-up energy gap in $NaCu_3Fe_2Os_2O_{12}$. *Inorg. Chem.* **2018**, *58*, 320−326, DOI: 10.1021/acs.inorgchem.8b02404.

https://doi.org/10.1021/acs.inorgchem.3c04243
Inorg. Chem. 2024, 63, 3499−3505